

UNCLASSIFIED

AD NUMBER	
AD029785	
CLASSIFICATION CHANGES	
TO:	unclassified
FROM:	confidential
LIMITATION CHANGES	
TO:	Approved for public release, distribution unlimited
FROM:	Distribution authorized to U.S. Gov't. agencies and their contractors; Administrative/Operational Use; 22 APR 1954. Other requests shall be referred to National Aeronautics and Space Administration, Washington, DC.
AUTHORITY	
NASA TR Server website; NASA TR Server website	

THIS PAGE IS UNCLASSIFIED

Armed Services Technical Information Agency

Because of our limited supply, you are requested to return this copy WHEN IT HAS SERVED YOUR PURPOSE so that it may be made available to other requesters. Your cooperation will be appreciated.

AD

29785

NOTICE: WHEN GOVERNMENT OR OTHER DRAWINGS, SPECIFICATIONS OR OTHER DATA ARE USED FOR ANY PURPOSE OTHER THAN IN CONNECTION WITH A DEFINITELY RELATED GOVERNMENT PROCUREMENT OPERATION, THE U. S. GOVERNMENT THEREBY INCURS NO RESPONSIBILITY, NOR ANY OBLIGATION WHATSOEVER; AND THE FACT THAT THE GOVERNMENT MAY HAVE FORMULATED, FURNISHED, OR IN ANY WAY SUPPLIED THE SAID DRAWINGS, SPECIFICATIONS, OR OTHER DATA IS NOT TO BE REGARDED BY IMPLICATION OR OTHERWISE AS IN ANY MANNER LICENSING THE HOLDER OR ANY OTHER PERSON OR CORPORATION, OR CONVEYING ANY RIGHTS OR PERMISSION TO MANUFACTURE, USE OR SELL ANY PATENTED INVENTION THAT MAY IN ANY WAY BE RELATED THERETO.

Reproduced by
DOCUMENT SERVICE CENTER
KNOTT BUILDING, DAYTON, 2, OHIO

CONFIDENTIAL

**NOTICE: THIS DOCUMENT CONTAINS INFORMATION AFFECTING THE
NATIONAL DEFENSE OF THE UNITED STATES WITHIN THE MEANING
OF THE ESPIONAGE LAWS, TITLE 18, U.S.C., SECTIONS 793 and 794.
THE TRANSMISSION OR THE REVELATION OF ITS CONTENTS IN
ANY MANNER TO AN UNAUTHORIZED PERSON IS PROHIBITED BY LAW.**

CONFIDENTIALCopy
RM L53L23NACA RM L53L23
AD No. 284215
ASTIA FILE COPY

RESEARCH MEMORANDUM

EXPERIMENTAL INFLUENCE COEFFICIENTS FOR THE DEFLECTION
OF THE WING OF A FULL-SCALE, SWEEP-WING BOMBER

By Alton P. Mayo and John F. Ward

Langley Aeronautical Laboratory
Langley Field, Va.

CLASSIFIED DOCUMENT

This document contains information affecting the National Defense of the United States within the meaning of the Espionage Laws, Title 18, U.S.C., Sec. 793 and 794, the transmission or revelation of which in any manner to an unauthorized person is prohibited by law.

**NATIONAL ADVISORY COMMITTEE
FOR AERONAUTICS**

WASHINGTON

APRIL 1954

CONFIDENTIAL

54AA-284215

NATIONAL ADVISORY COMMITTEE FOR AERONAUTICS

RESEARCH MEMORANDUM

EXPERIMENTAL INFLUENCE COEFFICIENTS FOR THE DEFLECTION
OF THE WING OF A FULL-SCALE, SWEEP-WING BOMBER

By Alton P. Mayo and John F. Ward

SUMMARY

The results of deflection tests on the wing of a full-scale, swept-wing jet bomber are presented in the form of structural influence coefficients relating the deflection of a system of points on the wing to concentrated loads applied on the wing spars. The procedures used for determining the coefficients are presented.

The influence coefficients are used to determine the wing deflections under assumed flight conditions and wing twist under a specific system of concentrated torques. These calculated wing deflections are compared with experimental results obtained from static proof tests at the same loading conditions. Also presented are curves of twist in the streamwise direction due to concentrated loads applied along the wing one-quarter-chord line.

INTRODUCTION

In connection with current flight tests being conducted by the National Advisory Committee for Aeronautics with a Boeing B-47 airplane it is required to establish values of wing structural influence coefficients in order to analyze properly the flight data for aeroelastic effects. The use of experimental influence coefficients provides an easier approach to the analysis of the aeroelastic effects than the use of the more indirect and less accurate theoretical methods. Inasmuch as the influence coefficients are of general interest and published data for an actual wing are practically nonexistent, it was thought desirable to publish these data and illustrate some of the procedures necessary to adapt the data to almost any deflection analysis. Wing deflections are calculated using the influence coefficients, which are based on relatively small concentrated loads, and compared with deflections measured with large distributed loads during the static proof tests in order to establish the range of validity of the coefficients.

CONFIDENTIAL

AIRPLANE AND TESTS

The airplane used in the test was a Boeing B-47A, six-engine, jet bomber shown in figure 1. The main wing structure was a tapered box beam with two spars at 17 percent and 58 percent of the wing chord (see figs. 2 and 3 and table 1). For ease in applying loads normal to the wing, the tail of the airplane was elevated to bring the wing root chord into the horizontal plane. Loads were applied symmetrically on both wings in order to eliminate the necessity of providing rolling restraint at the airplane fuselage.

The loads were applied upward with hydraulic jacks through rectangular felt-covered loading pads, approximately 8 inches square, which had sufficient surface area to reduce localized skin deformations. Sensitive dynamometers were used to measure the concentrated loads applied. Loading points were located at the intersection of rib and spar center lines (see fig. 3), so as to take advantage of additional strength at these points and to correlate loading-point locations with known structural dimensions.

Wing deflections were measured by means of dial gages and hanging scales located symmetrically about the airplane center line on the front and rear spars at locations shown in figure 3. The reference plane for these measurements was the heavily reinforced floor of the Langley aircraft loads calibration laboratory which housed the airplane. Four dial gages were mounted above the wing attachment fittings to establish corrections for any movement of the airplane fuselage after the initial gage readings were recorded. Dial gages, supported on tripod stands were used at deflection stations 9 to 16 and hanging scales were used at stations 1 to 8. The hanging scales were read with a surveyor's transit set up beneath the airplane tail. The distance from the transit to the scales was approximately 60 feet. Test procedures were the same for all loading points with every deflection gage being read at each change in load magnitude or location (see fig. 3).

The net concentrated loads used increased in magnitude from 2,000 pounds at the wing tip to 20,000 pounds at the root (see fig. 3). In order to eliminate effects of structural slippage, a tare load of 20 percent of the station maximum load was applied at each station. All subsequent data taken was adjusted so as to be the incremental values from the 20-percent-tare-load condition. These adjusted gage readings are referred to as deflection readings for the rest of this paper. The concentrated loads were applied and relieved in 20-percent increments in order to provide a more thorough check on gage behavior.

ACCURACY OF MEASUREMENTS AND CORRECTION FOR AIRPLANE MOVEMENT

The dial gages used to measure the deflections at gage stations 9 to 20, inclusive (see fig. 3) were graduated and read to 0.001 inch with an estimated overall accuracy of ± 0.001 inch. The hanging scales used had graduations of 0.050 inch and the overall estimated accuracy of the scale readings was ± 0.050 inch. The accuracy of the loads applied was estimated to have been ± 5 pounds. The centers of load and gage locations were estimated to be within ± 1.0 inch of the locations given in figure 3.

During the application of the point loads, the airplane was slightly pitched, rolled, and displaced vertically, thus changing the zero readings of the four root gages used as reference points.

The corrections for airplane movement were based on the four root gages, 17 and 18 on each wing (see fig. 3). The corrections applied to the individual deflection readings at a point P expressed in terms of the deflection of the four root gages were:

Roll:

$$\Delta Z_P = \frac{1}{2} \left(\frac{Z_{18R} - Z_{18L}}{91.2} + \frac{Z_{17R} - Z_{17L}}{88.0} \right) Y_P \quad (1)$$

(where positive values of Y correspond with the left wing and negative values of Y correspond with the right wing)

Pitch:

$$\Delta Z_P = \frac{1}{2} \left(\frac{Z_{17L} - Z_{18L}}{80.9} + \frac{Z_{17R} - Z_{18R}}{80.9} \right) X_P \quad (2)$$

Vertical displacement:

$$\Delta Z_P = \frac{1}{2} \left[1.204 (Z_{18L} + Z_{18R}) - 0.204 (Z_{17L} + Z_{17R}) \right] \quad (3)$$

The above equations are deduced from the root-deflection gage locations shown in figure 3.

INFLUENCE COEFFICIENTS AND CURVES

The deflection readings, corrected as in the foregoing section, were converted to influence coefficients, which relate the deflection of a system of points on the two spars to concentrated loads applied along these spars. In order to obtain an influence coefficient, the corrected deflection data for a given deflection station were plotted against the net load applied at a given load station and a line faired through the points. The influence coefficient is the slope of the line. Figure 4 shows a typical result obtained for the deflection at station 2 on the left wing as the load is applied at station 42 on the left wing. The scattering of the uncorrected points in this figure illustrates the necessity of including the corrections for airplane movement. When the data are corrected, the slope of the load-deflection curve shows good agreement at all points, implying a linear relation between deflection and load.

In general, individual plots were not made to obtain influence coefficients. Instead, the original data were inserted into the IBM calculator, which was set up to give influence coefficients based on a least-squares analysis of the data and which included the corrections required for airplane movement.

The coefficients were obtained in terms of deflections in inches at the deflection stations per 1,000 pounds at the load stations. Influence coefficients obtained in this manner are given in table 2 for the left wing and table 3 for the right wing.

It may be noted in table 2 that the deflection at station 2 with 1,000 pounds at station 42 is 2.2744 while from figure 4 the corresponding value is 2.27 as close as can be read.

Figure 5 shows a typical influence-coefficient curve for the deflection at station 6 on the left front spar due to 1,000 pound loads at various positions along the front and rear spars of the left wing. The curves shown were plotted directly from table 2. A curve of this type is particularly useful when it is required to determine the deflection at a tabulated deflection station due to loadings distributed along the span. Since any load distribution on the wing can be considered to be divided into distributed loads on the front and rear spars if the chordwise centers of pressure are known, the station deflection may be determined by either of two methods. The distributed loads along the spars can be replaced by equivalent concentrated loads which in turn are multiplied by the influence coefficients corresponding to the loading stations. The deflections at the station for each of the concentrated loads are added to give the total deflection under the original load distribution.

CONFIDENTIAL

Alternately, the curves of spar load distribution can be multiplied by the influence-coefficient curve for the station to obtain a product curve which is then integrated to obtain the deflection at that station.

Although the data presented in tables 2 and 3 are considered the basic data of this report, the application of this type of data to a specific analysis may call for influence coefficients at stations other than those tabulated.

In order to obtain influence coefficients for stations on the wing spars but not at deflection stations tabulated, it is necessary to plot several deflection curves for a 1,000-pound load at a different spar station in each case. This has been done in figure 6 as an example. Influence-coefficient curves are then plotted from values of deflection at the station in question (see fig. 7). In order to obtain influence coefficients for deflection stations off the spars, it is necessary to determine the influence coefficients for the front and rear spars at the same spanwise location and interpolate between them.

Another type of interpolation which can be made directly with apparently little error in the results is to use Maxwell's Law of Reciprocal Deflections in which the loading and deflection stations are interchanged. A demonstration of this law applied to present data is shown in figure 8. The data used in figure 8 were obtained by constructing influence-coefficient curves for each deflection station and reading values at all other deflection stations. A given point on the plot is the result of choosing two arbitrary deflection stations P and Q and plotting the deflection at P, due to a 1,000-pound load at Q, against the deflection at Q, due to a load at P.

From the basic data given in tables 2 and 3 other types of influence coefficients can be derived to suit any particular analytical procedure. One type of influence-coefficient curve which will be particularly useful in the analysis of flight data for a Boeing B-47 is a curve of streamwise twist induced by airloads acting along the quarter-chord line. Figure 9 shows these curves of streamwise twist for 1,000-pound point loads on the quarter chord at various stations along the span. The points are retained in figure 9 to show the scatter and fairing required.

COMPARISONS

The influence coefficients were obtained with concentrated loadings which, while high on a pounds-per-square-foot basis, were relatively low on a total loads basis. Since the influence-coefficient results are expected to be used with larger distributed loads, where nonlinearities may exist, a number of comparisons are made between deflections determined

CONFIDENTIAL

from the influence coefficients and deflections obtained from static proof tests at high-load levels.

Figure 10 shows a comparison between the deflection of the front and rear spars measured in a static proof test of a Boeing B-47B wing (ref. 1) and deflections computed through the use of experimental influence coefficients using similar loading conditions. The equivalent concentrated spar loads used to duplicate actual proof-test loading conditions are given in table 4. The Boeing B-47B wing differs primarily from the B-47A wing in the skin thickness near the root.

Another comparison is shown in figure 11 where the deflection resulting from a 8,000-pound concentrated load on the XB-47 wing (ref. 2) is compared with results obtained with influence coefficients from the B-47A. The B-47A wing is basically similar to the XB-47 wing except for the substitution of forged fittings in place of machined fittings.

In still another test described in reference 1 a B-47B wing is subjected to three large concentrated torque loads and the wing twist measured. The front and rear spar deflections of the B-47A wing under similar torques as determined from the influence coefficients of this report are shown in figure 12. The spar deflections in figure 12 were found to be somewhat erratic, because the influence coefficients used to obtain these deflections were determined with loadings which contained very small torque components. This resulted in a loss of accuracy which is evident from the scatter in figure 12. Least-squares parabolic curves were passed through the points which assume zero deflection at the wing attachment fittings. The twists derived from the least-squares curves are compared in figure 13 with B-47B data from reference 1.

Calculations of the tip deflections made in reference 3, using the EI distribution of the B-47B for an assumed in-flight loading condition, resulted in a tip deflection of 87 inches, whereas, the tip deflection computed by the influence coefficients contained herein gave a deflection of 82 inches (see fig. 10).

DISCUSSION

In order to provide a check on original data, the uncorrected and corrected data for each gage station were plotted. The station-deflection curve shown in figure 4 is typical of about 90 percent of the data with regard to scatter of the final corrected points and linearity of the curves. It is typical of all the data in indicating the need for including corrections due to movements of the airplane during load application. In the cases not typified by figure 4, a few of the data points were erratic due to reading and recording errors during the test.

CONFIDENTIAL

Influence curves, for a particular deflection station due to loading along the spars, resulted in fair curves with very little scatter. As might be expected, the curves showing wing twist, in planes perpendicular to the elastic axis derived from small differential deflections of the spars show a great deal of scatter as is evidenced in figure 12. Because of this scatter the twist curves shown in figure 13 are only a general comparison and the results cannot be considered conclusive as to the relative stiffnesses of the B-47A and B-47B wings. In the twist curves for loads along the quarter-chord line in figure 9, the streamwise component of the twist perpendicular to the elastic axis is secondary to the twist in the streamwise direction due to bending. The smallness of the scatter shown in figure 9 is due to the fact that the streamwise twist was obtained from large differential spar deflections mainly due to wing bending which could be determined with fair accuracy. In connection with figure 9 it is to be noted that for the outboard stations the twist continues to increase outboard of the loading point, which is not in agreement with elementary beam theory. This discrepancy cannot be fully accounted for by possible inaccuracies in measurement and is assumed to be due to secondary stress carryover into the outboard portion of the wing and to differences in the slopes of the front and rear spars at the streamwise loading station.

The data in figure 9 correspond to the structural matrix $[S_2]$ in equation (14) of reference 4. The required values to be inserted in the matrix may be read from the figure taking proper account of the units involved. The twist curves of figure 9 are for eight equally spaced stations; similar curves for any other system of stations may be obtained from cross-plotting of the curves given.

Although the influence coefficients given were obtained under conditions with no chordwise forces present, such forces should be included in the most accurate calculations for wing twist. The inclusion of chordwise forces is in the nature of a correction. The necessity arises because the chordwise forces acting on the deflected wing produce a torque distribution along the span. This torque distribution may be duplicated for use with influence-coefficients methods by application of couples through superimposed spar loads. In the comparisons given in figure 10, the effect of chordwise force on the deflected wing has been included in the calculation of deflections by influence coefficients so as to agree with the chordwise force effects present in the proof-test deflections. In the comparisons shown in figures 11 and 13 no corrections for chordwise forces were necessary.

From the comparisons shown in figures 10 and 11 it appears that there is apparently little difference in the deflection characteristics of the Boeing B-47A and B-47B wings. More important, however, is the indication that the influence-coefficient results obtained with relatively small point loads can apparently be extended to the maximum loading conditions to be expected in flight. Further confidence in the influence coefficients

and in the ability to analyze the flight results arises from the fact that Maxwell's Law of Reciprocal Deflections (see fig. 8) is checked very well by deflection measurements.

Langley Aeronautical Laboratory,
National Advisory Committee for Aeronautics,
Langley Field, Va., December 3, 1953.

REFERENCES

1. Parsons, Cecil E.: Wing Destruction Tests - Model B-47B. Test No. T-25299 (Contract No. W33-038 ac-22413), Boeing Airplane Co. (revised Apr. 14, 1951).
2. Spengler, C. J.: Torsional and Bending Stiffness Tests of Wing. [Model B-47.] Test No. T-25330 (Contract No. W33-038 ac-22413), Boeing Airplane Co., Jan. 17, 1949.
3. Nelson, Melvin A.: Wing Stress Analysis. [Model B-47B.] Vol. I. Document No. D-10207 (Contract No. W33-038 ac-22413), Boeing Airplane Co., Apr. 10, 1950.
4. Gray, W. L., and Schenk, K. M.: A Method for Calculating the Subsonic Steady-State Loading on an Airplane With a Wing of Arbitrary Plan Form and Stiffness. NACA TN 3030, 1953.

TABLE 1.- PERTINENT WING AND NACELLE CHARACTERISTICS

Sweepback of 25-percent-chord line, deg	35
Sweepback of elastic axis, deg	34.12
Front spar center line, percent chord	17
Rear spar center line, percent chord	58
Elastic axis (assumed), percent chord	38
Thickness ratio	0.12
Horizontal distance from elastic axis forward to nacelle center of gravity, in.:	
Inboard nacelle	123.1
Outboard nacelle	17.5
Vertical distance from elastic axis to nacelle center of gravity, in.:	
Inboard nacelle	55
Outboard nacelle	----
Nacelle deadweight, lb:	
Inboard nacelle	7,566
Outboard nacelle	3,251

TABLE 2.- DEFLECTION INFLUENCE COEFFICIENTS FOR LEFT WING

Deflection stations	Deflection influence coefficients, in./1,000 lb, for load stations -														
	21	22	41	42	61	62	81	82	101	102	121	122	161	162	302
1	2.9688	3.1926	2.1232	2.4577	1.3000	1.5773	0.8769	1.0940	0.5447	0.7163	0.3512	0.4358	0.0879	0.1340	0.0451
2	2.9130	2.9334	2.0163	2.2744	1.2539	1.4742	.8582	1.0178	.5344	.6747	.3440	.4148	.0808	.1267	.0425
3	2.4271	2.5031	1.7695	2.0030	1.1109	1.3327	.7575	.9402	.4849	.6266	.3105	.3871	.0818	.1186	.0402
4	2.2705	2.2250	1.6420	1.8557	1.0704	1.2478	.7466	.8863	.4726	.5927	.3055	.3661	.0800	.1124	.0377
5	1.6003	1.6283	1.2402	1.3822	.9368	.9859	.5927	.7159	.3828	.4934	.2458	.3090	.0658	.0985	.0335
6	1.4836	1.4930	1.1565	1.2579	.8048	.9070	.5761	.6569	.3664	.4620	.2429	.2918	.0671	.0915	.0300
7	1.1083	1.1763	.9251	1.0085	.6392	.7609	.4915	.5831	.3148	.4105	.2078	.2633	.0533	.0876	.0287
8	.9732	1.0084	.8340	.8736	.6081	.6709	.4692	.5741	.2959	.3690	.2042	.2367	.0550	.0763	.0260
9	.7258	.8079	.6325	.7018	.4672	.5331	.3511	.4415	.2428	.3231	.1713	.2063	.0483	.0701	.0237
10	.6483	.6650	.5694	.5734	.4026	.4444	.3313	.3690	.2289	.2772	.1604	.1765	.0466	.0618	.0205
11	.5235	.5282	.4349	.4677	.3290	.3699	.2600	.3004	.1869	.2394	.1328	.1647	.0380	.0574	.0195
12	.4198	.4225	.3578	.3760	.2796	.3024	.2278	.2422	.1699	.1939	.1255	.1349	.0379	.0490	.0174
13	.1783	.1896	.1588	.1729	.1285	.1412	.1044	.1179	.0405	.1017	.0632	.0753	.0215	.0311	.0114
14	.1268	.1302	.1154	.1192	.0927	.0970	.0811	.0804	.0620	.0694	.0510	.0504	.0205	.0238	.0102
15	.0653	.0760	.0545	.0649	.0460	.0554	.0336	.0402	.0327	.0390	.0264	.0323	.0117	.0180	.0080
16	.0403	.0468	.0370	.0379	.0317	.0322	.0264	.0252	.0259	.0230	.0193	.0195	.0122	.0096	.0041
17	.0003	-.0003	.0007	.0004	.0007	.0003	.0008	.0006	.0007	-.0006	-.0003	.0002	.0002	.0002	-.0001
18	.0003	-.0016	.0005	-.0001	.0001	-.0004	-.0001	-.0001	-.0003	-.0008	-.0005	.0000	-.0001	.0000	.0000
19	-.0032	-.0014	-.0016	-.0015	-.0013	-.0009	-.0015	-.0010	-.0011	-.0009	-.0013	.0002	-.0010	.0000	-.0001
20	-.0027	-.0023	-.0021	-.0027	-.0022	-.0017	-.0021	-.0016	-.0012	-.0010	-.0017	-.0005	-.0007	-.0004	-.0002

TABLE 3.- DEFLECTION INFLUENCE COEFFICIENTS FOR RIGHT WING

Deflection stations	Deflection influence coefficients, in./1,000 lb, for load stations -															302
	21	22	41	42	61	62	81	82	101	102	121	122	161	162	201	202
1	3.0958	3.2214	2.0961	2.4423	1.3168	1.5551	0.8837	1.0852	0.5628	0.7137	0.3553	0.4532	0.0972	0.1372	0.0358	0.0529
2	2.9083	3.0083	2.0092	2.2542	1.2767	1.4594	.8585	1.0251	.5564	.6763	.3536	.4257	.0967	.1299	.0366	.0518
3	2.4256	2.5734	1.7437	1.9829	1.1259	1.3215	.7668	.9388	.4946	.6245	.3167	.3995	.0898	.1221	.0317	.0474
4	2.2438	2.4180	1.6672	1.8555	1.0935	1.2407	.7371	.8849	.4929	.5877	.3114	.3786	.0883	.1162	.0227	.0430
5	1.5833	1.7498	1.2229	1.3797	.8499	.9847	.5936	.7198	.3964	.4932	.2543	.3226	.0752	.1016	.0261	.0399
6	1.4661	1.5584	1.1506	1.2517	.8093	.9011	.5736	.6639	.3894	.4467	.2523	.2997	.0741	.0947	.0264	.0370
7	1.1687	1.2423	.9203	1.0199	.6615	.7655	.4848	.5843	.3300	.4120	.2128	.2747	.0640	.0876	.0221	.0332
8	1.0110	1.0692	.8465	.8778	.6112	.6592	.4510	.5175	.3162	.3662	.2069	.2397	.0628	.0796	.0233	.0312
9	.7823	.8174	.6415	.7013	.4782	.5376	.3704	.4393	.2603	.3256	.1759	.2171	.0503	.0694	.0183	.0269
10	.6433	.6734	.5406	.5835	.4184	.4489	.3329	.3649	.2437	.2736	.1664	.1863	.0498	.0640	.0196	.0253
11	.5155	.5350	.4268	.4679	.3277	.3854	.2594	.3009	.1910	.2386	.1332	.1491	.0422	.0585	.0142	.0211
12	.4267	.4296	.3548	.3733	.2770	.2927	.2233	.2412	.1732	.1923	.1264	.1386	.0426	.0501	.0154	.0195
13	.1865	.1979	.1612	.1736	.1284	.1409	.1050	.1189	.0789	.1020	.0652	.0767	.0252	.0318	.0082	.0119
14	.1393	.1358	.1120	.1188	.0923	.0971	.0799	.0815	.0620	.0690	.0503	.0523	.0246	.0242	.0101	.0104
15	.0883	.0872	.0624	.0704	.0527	.0573	.0489	.0486	.0351	.0385	.0273	.0357	.0149	.0178	.0051	.0064
16	.0618	.0516	.0395	.0479	.0362	.0385	.0345	.0302	.0260	.0270	.0200	.0209	.0126	.0090	.0066	.0050
17	.0012	.0000	.0003	-.0004	.0003	.0004	.0001	.0001	-.0001	-.0006	-.0002	.0005	.0002	.0004	-.0011	.0002
18	.0006	.0013	.0006	.0008	.0007	.0004	.0004	.0005	.0001	-.0005	-.0003	.0002	.0002	.0001	-.0008	.0006
19	-.0006	-.0011	-.0014	-.0034	-.0007	-.0089	-.0001	-.0003	-.0010	-.0010	-.0014	-.0003	-.0002	-.0001	-.0005	.0000
20	-.0009	-.0005	-.0014	-.0011	-.0011	-.0010	-.0004	-.0009	-.0009	-.0016	-.0012	-.0006	-.0006	-.0005	-.0005	.0000

TABLE 4.- EQUIVALENT CONCENTRATED SPAR LOADS
FOR PROOF-TEST CONDITIONS

Elastic axis station, in.	Front spar loading, lb	Rear spar loading, lb
821	2,128	1,081
777	2,147	510
732	3,509	899
692	4,119	1,048
685	-----	-8,740
658	2,116	-----
652	5,040	367
612	4,694	1,166
573	4,717	1,142
532	5,048	1,278
492	5,811	1,381
452	5,936	1,456
414	6,344	914
376	5,328	1,332
343	-----	-14,536
342	5,274	1,318
308	5,308	1,351
304	-30,116	-----
270	6,019	1,639
235	6,612	1,778
198	7,137	2,119
163	7,086	2,104
128	7,406	2,249
93	6,323	1,867
70	4,794	0
57	3,796	0

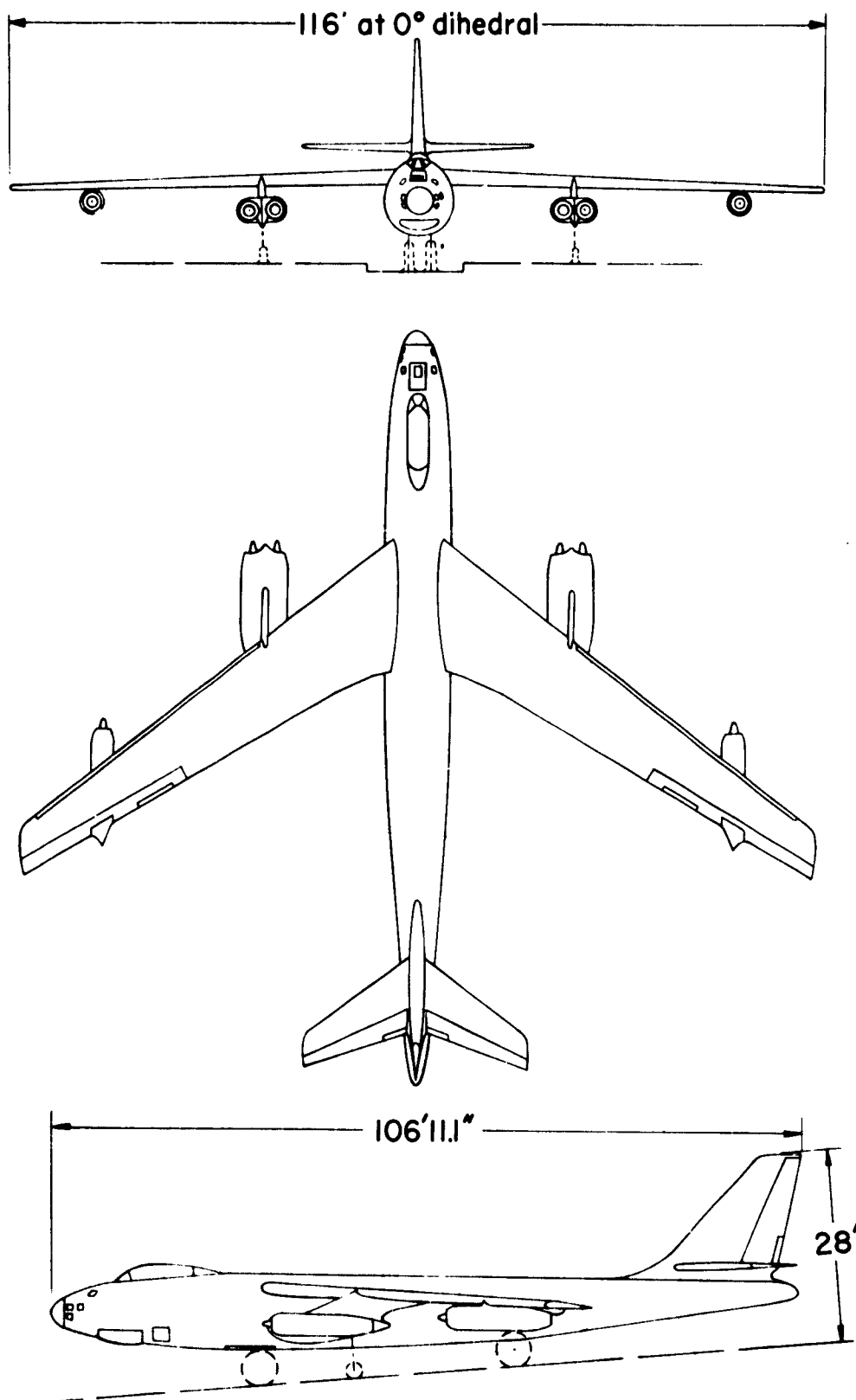


Figure 1.- Three views of test airplane.

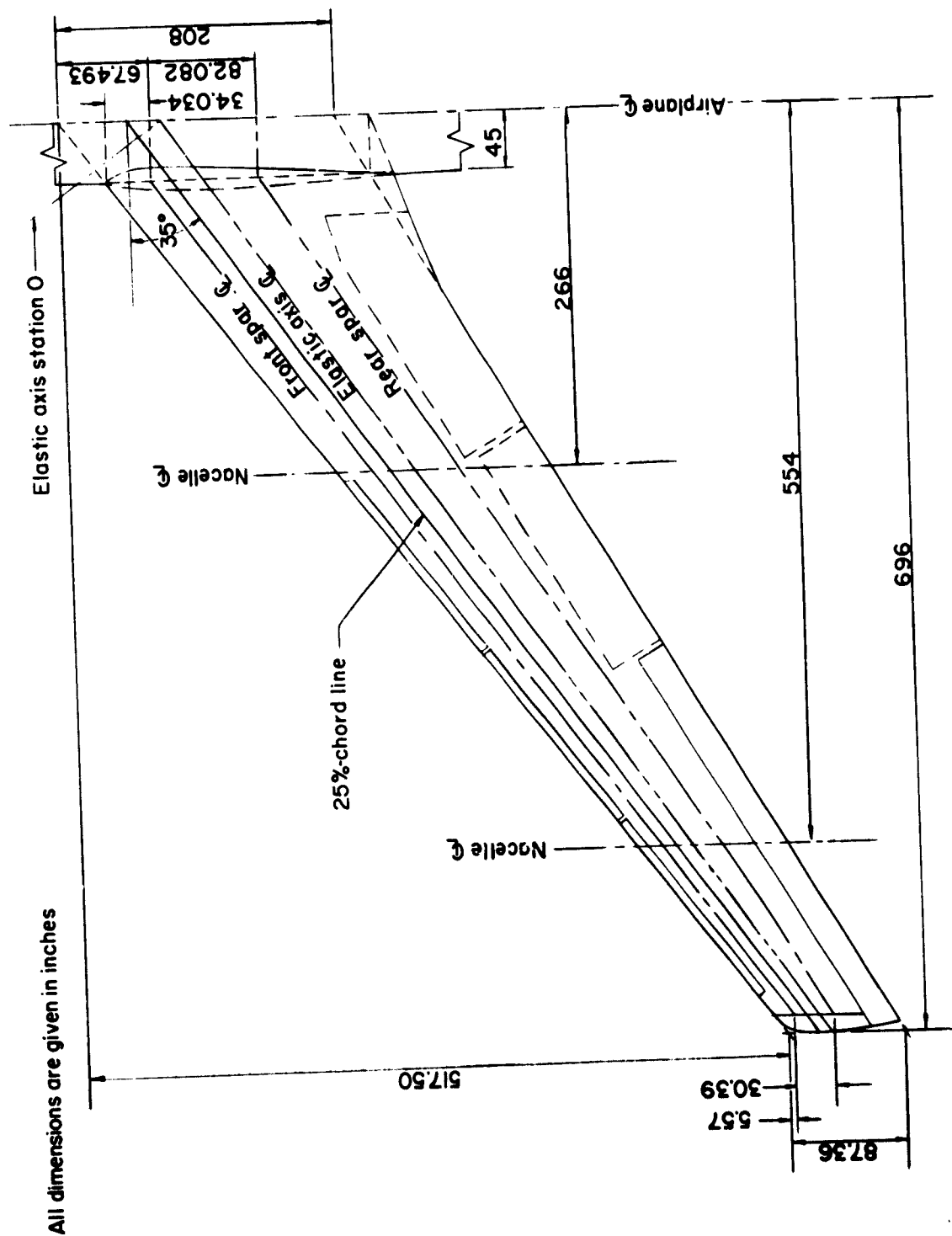


Figure 2.- Wing plan-form geometry used in wing deflection calculations.

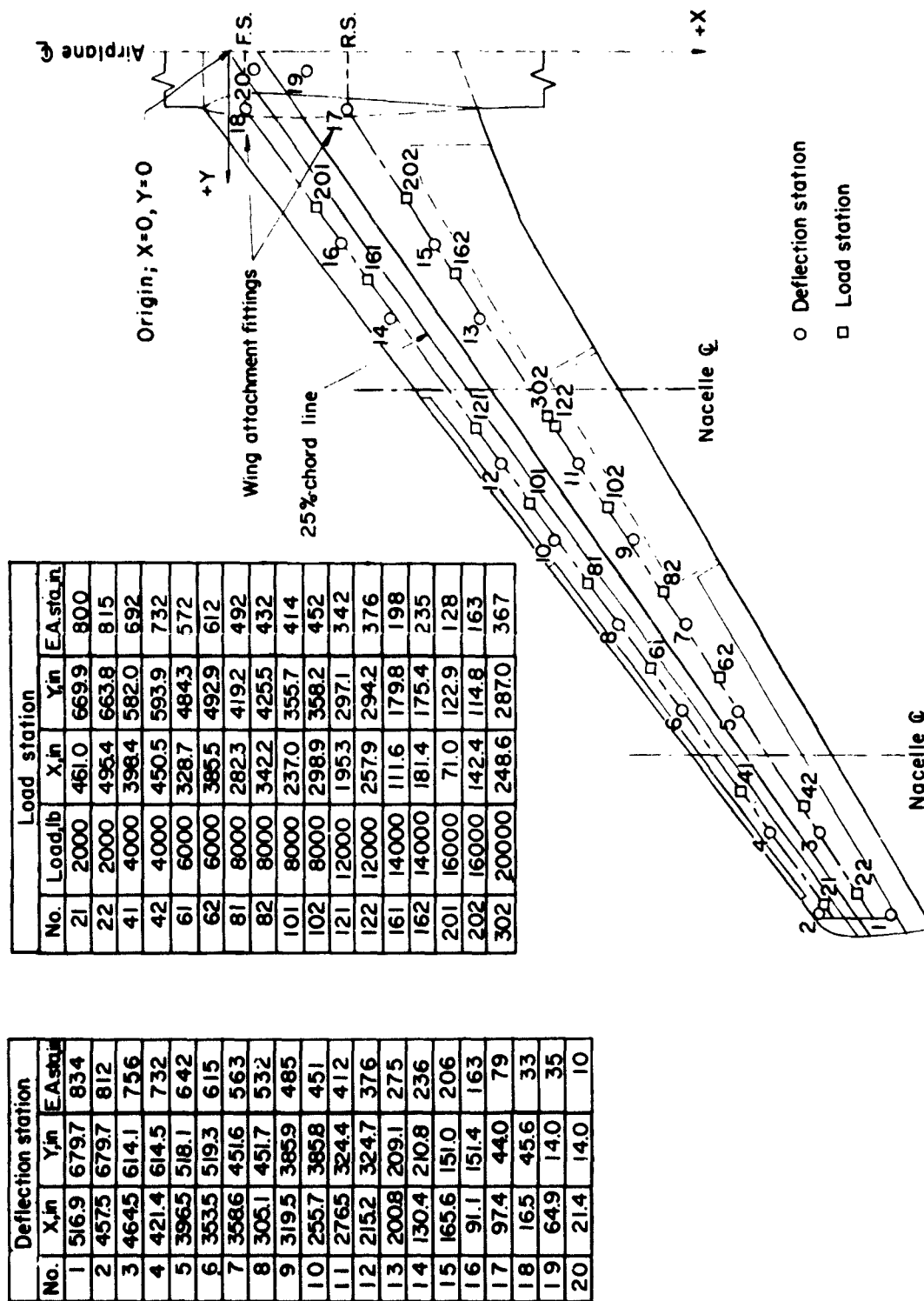


Figure 3.-- Locations on wing of load stations and gage stations used during test and magnitude of loads applied.

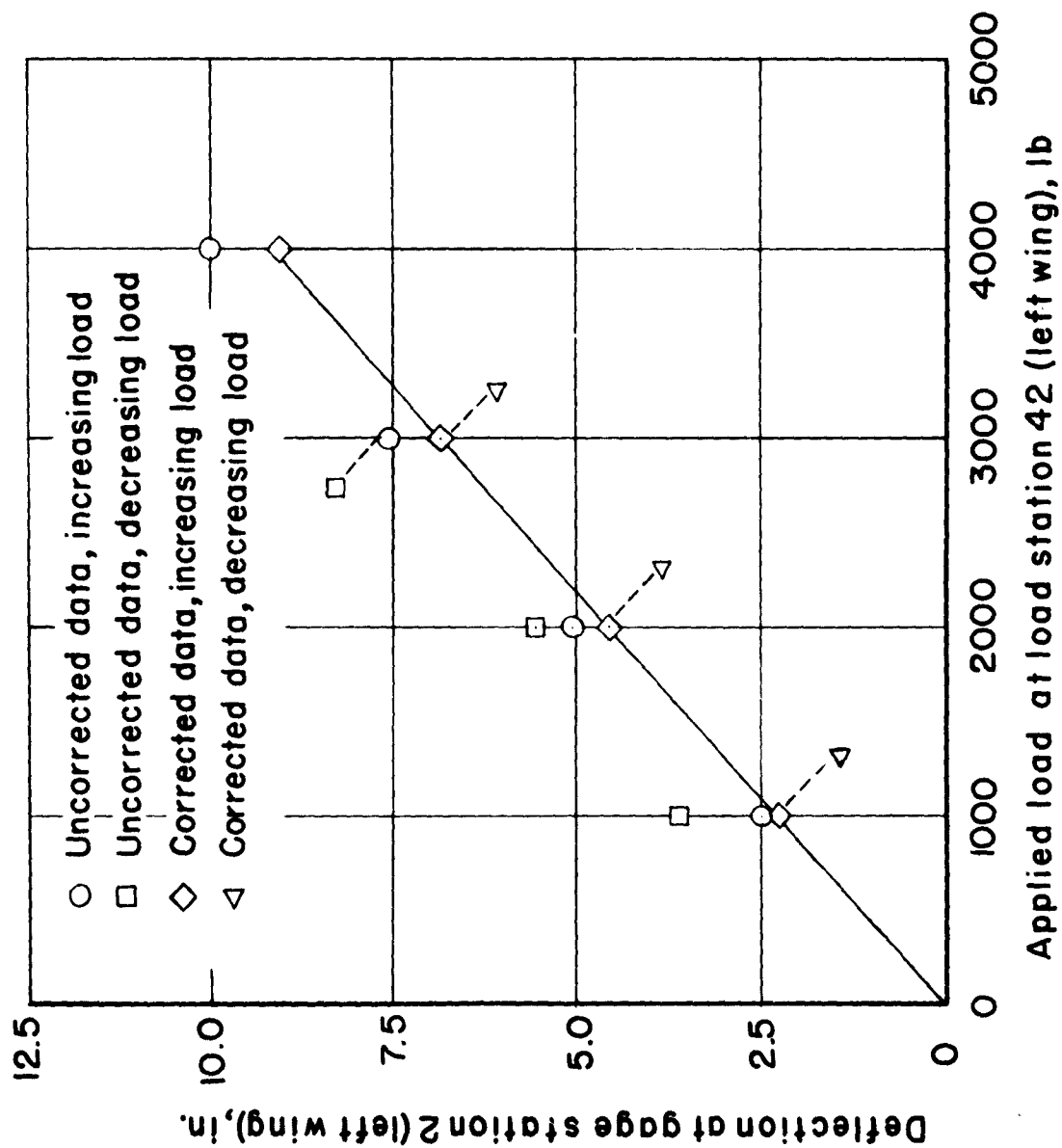


Figure 4.- A typical station deflection with load.

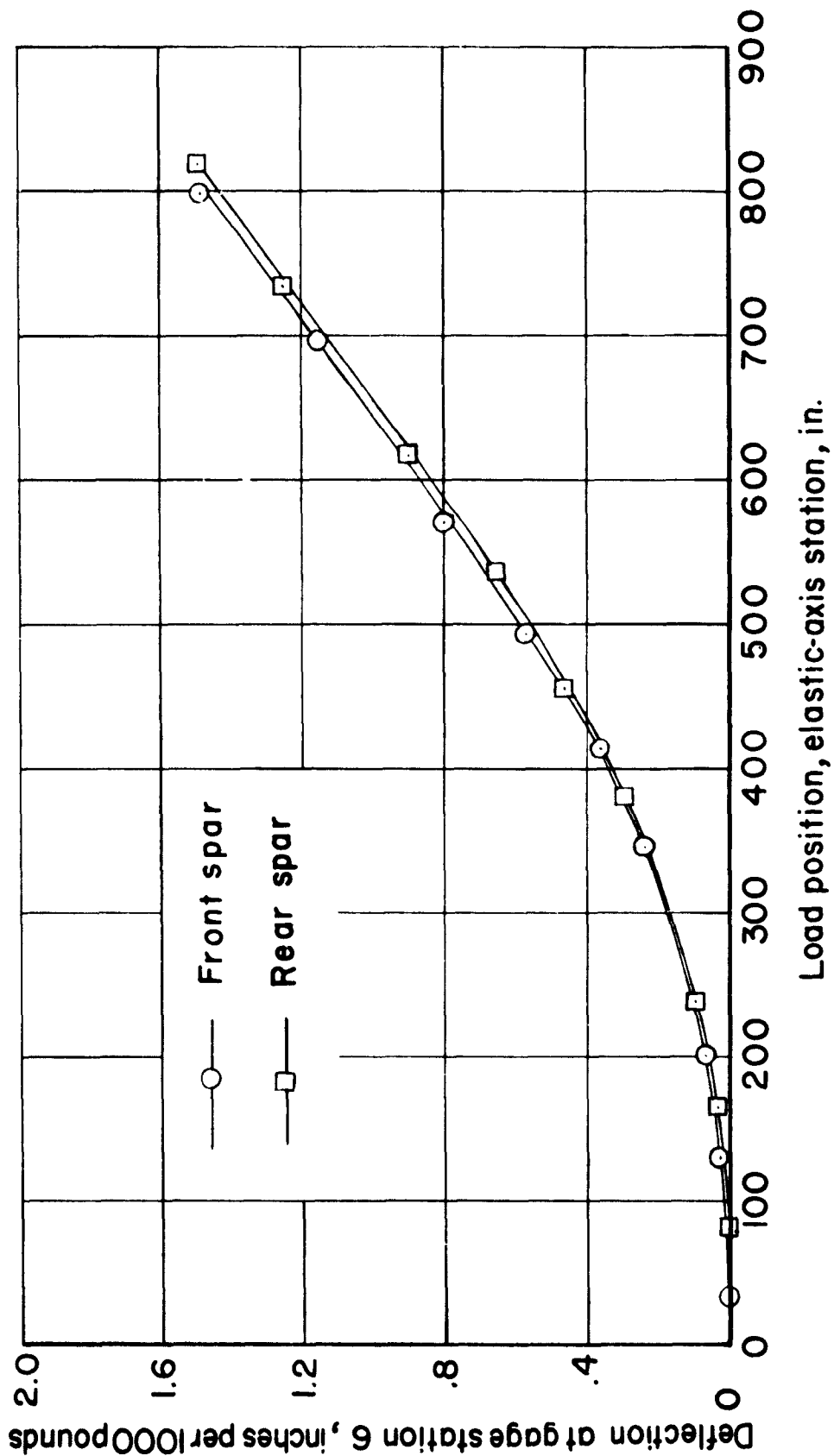


Figure 5.- A typical influence-coefficient curve showing the deflection of a station with changes in load position along spars.

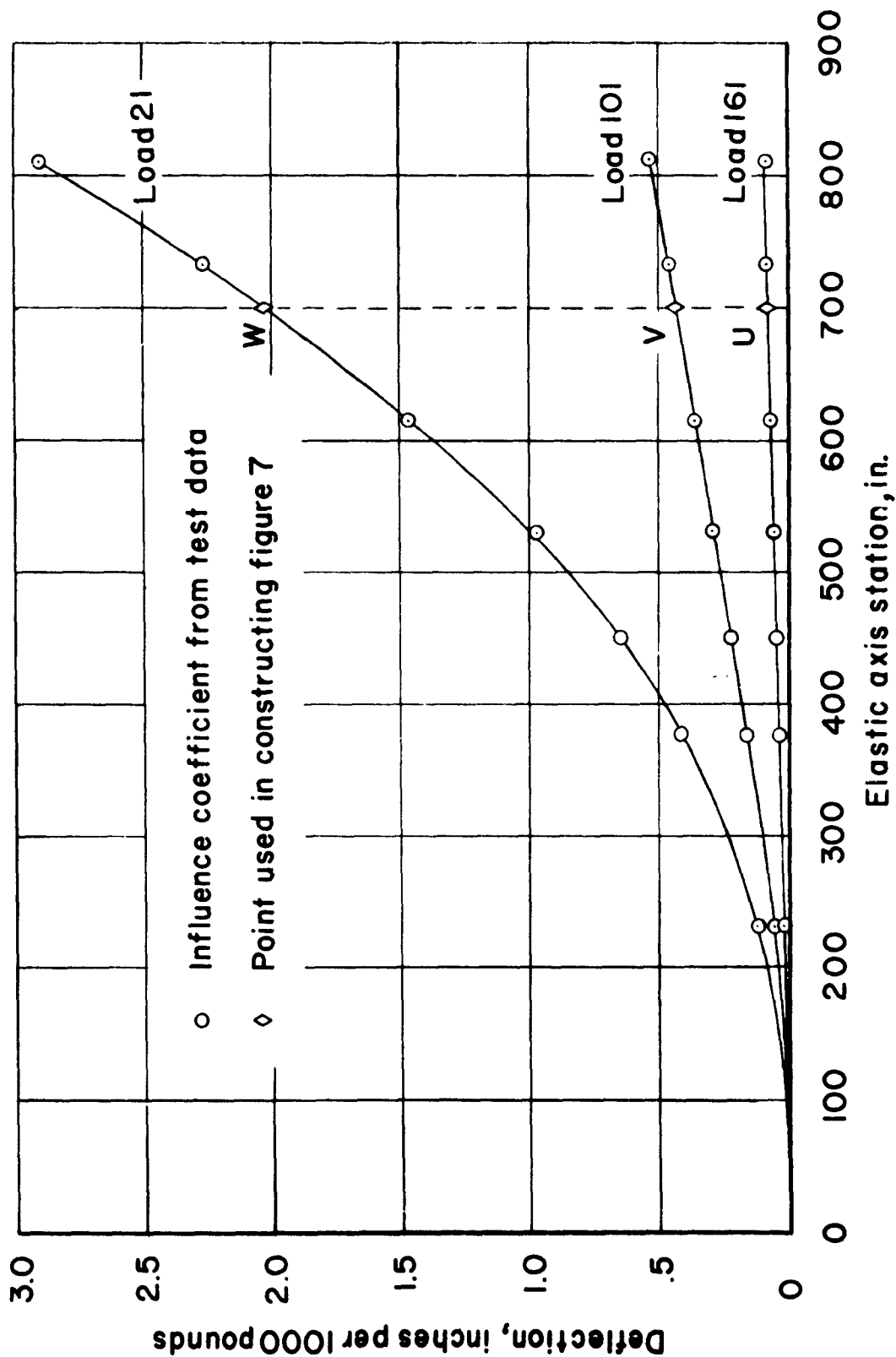


Figure 6.- Typical front-spar deflection curves for 1000-pound loads applied at various spanwise stations.

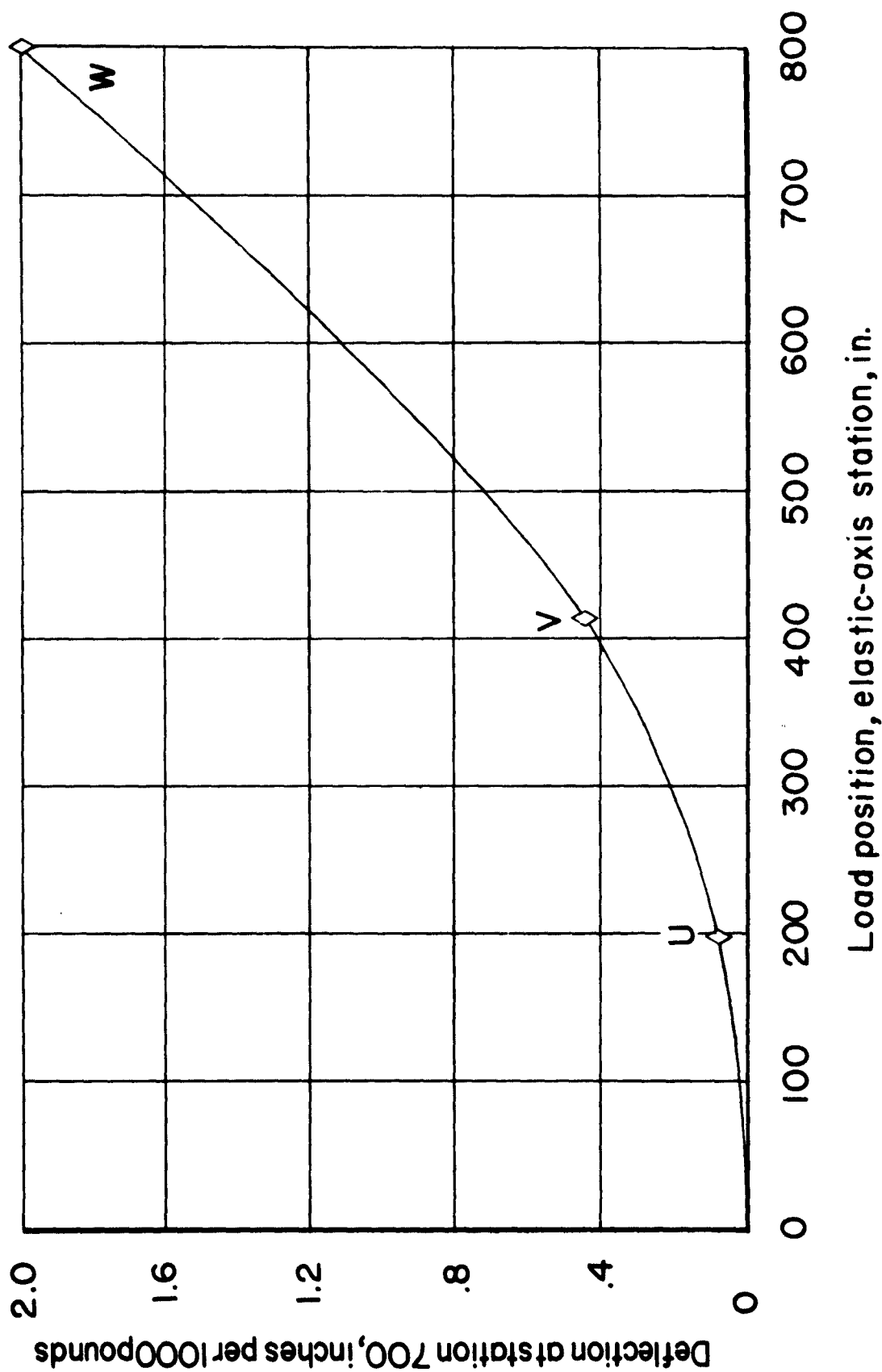


Figure 7.- Influence-coefficient curve for a point on the wing where no deflection gage was located.

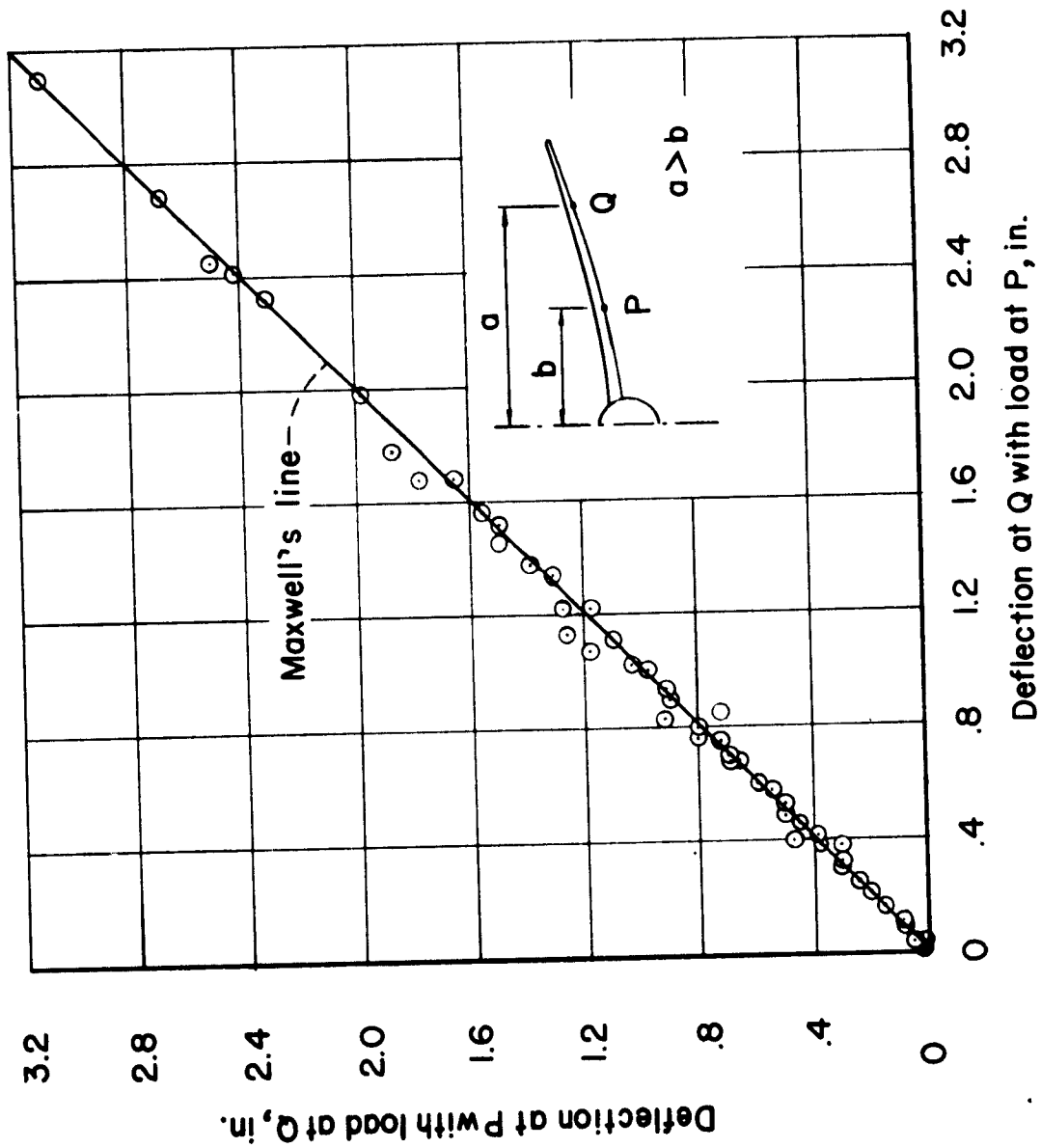


Figure 8.- Comparison of experimental data with Maxwell's Law of Reciprocal deflections.

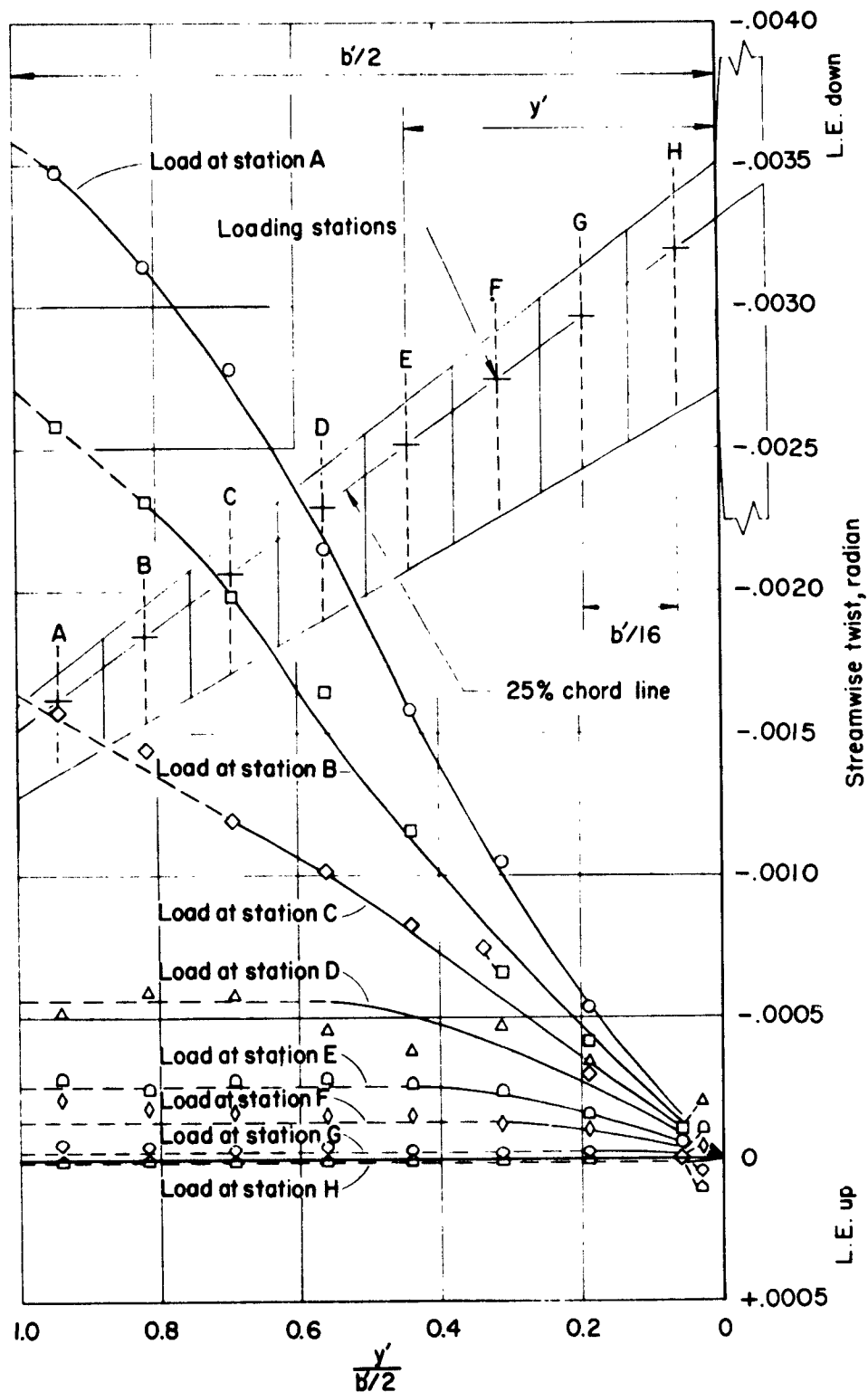


Figure 9.- Twist of wing in planes parallel to the airplane center line due to 1000-pound point loads applied at various stations along wing 25-percent-chord line.

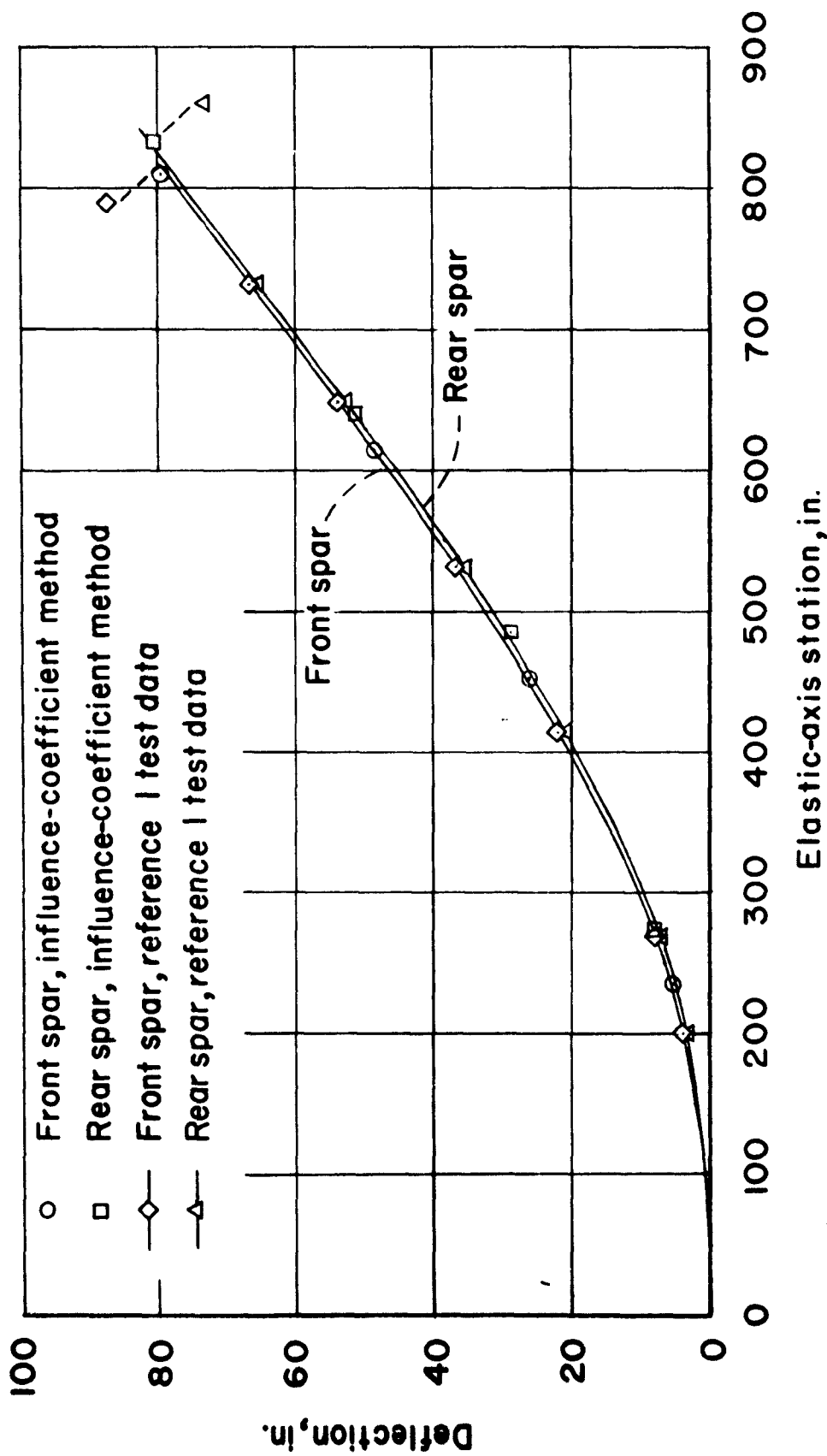


Figure 10.- Wing deflections due to application of point loads representing a proof-loading condition.

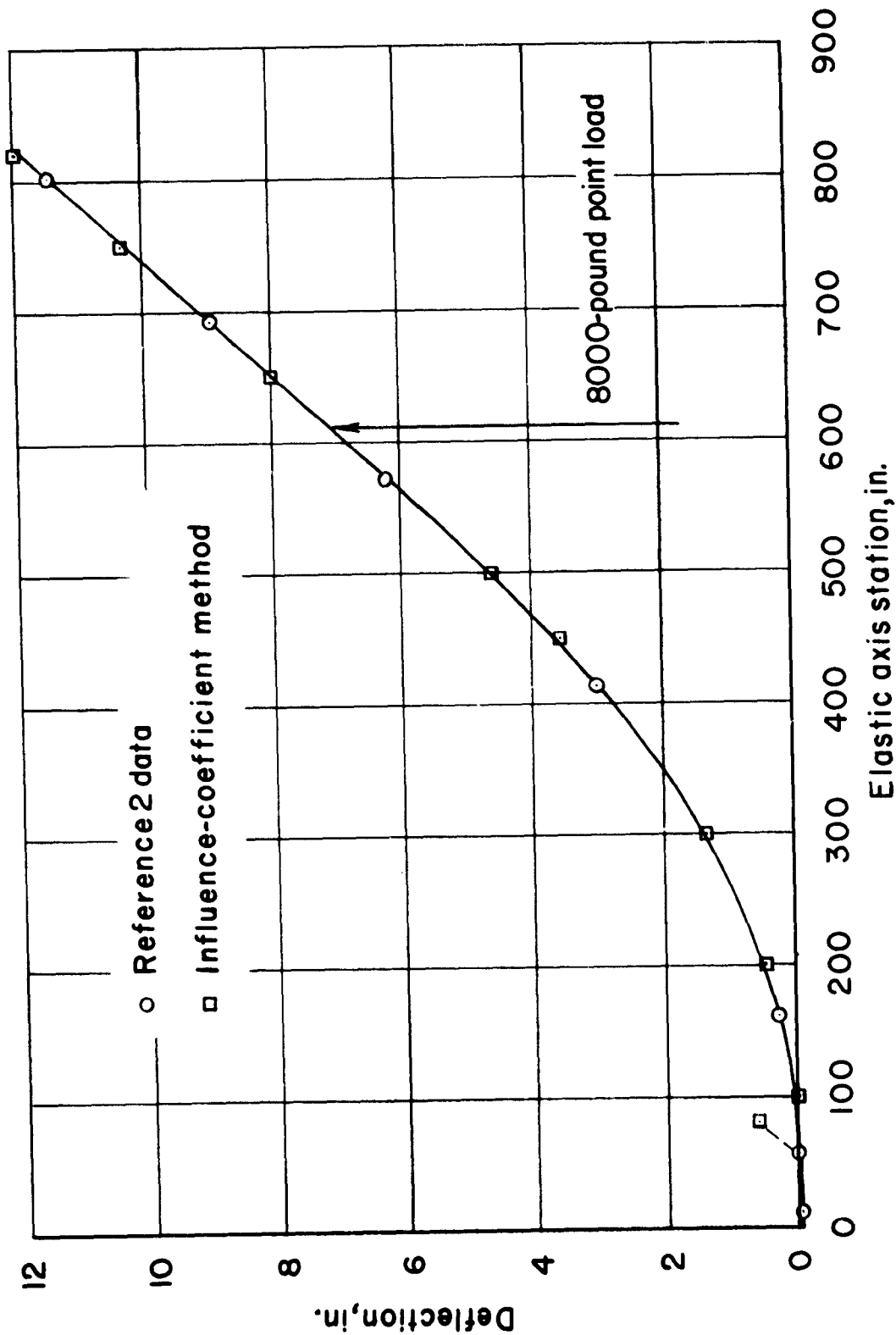


Figure 11.-- Deflection of wing elastic axis with an 8000-pound point load applied on elastic axis at station 612.

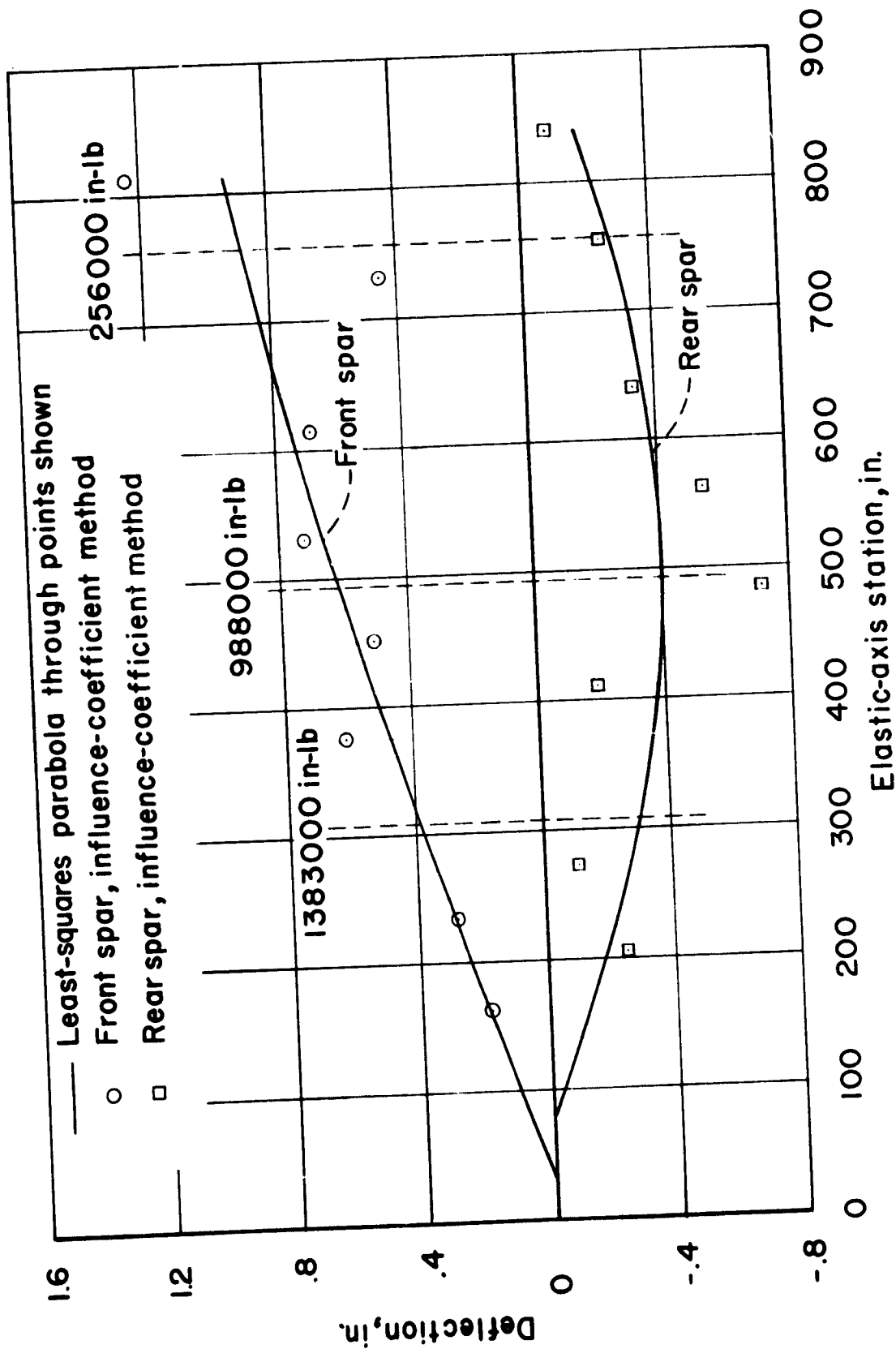


Figure 12.- Deflection of spars due to three concentrated torques applied in planes perpendicular to wing elastic axis.

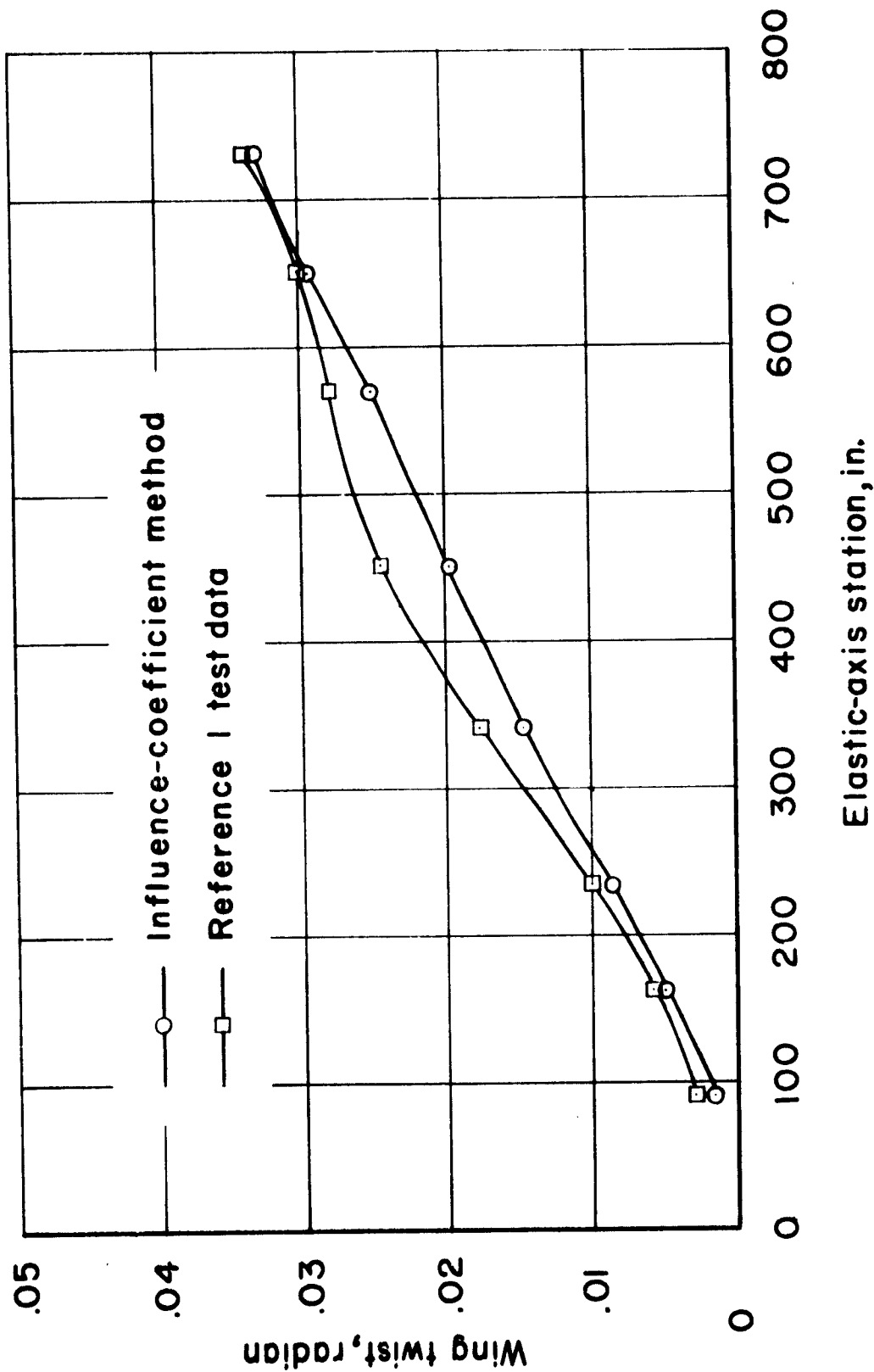


Figure 13.- Twist of wing in planes perpendicular to elastic axis due to three concentrated torques applied in planes perpendicular to wing elastic axis.